

Contents

1	The problem (Reisenegger 2017)	2
1.1	PDF and initial conditions	2
1.2	First step. Solving for velocities	2
1.3	Second step. Solving for poloidal perturbation	4
1.4	Third step. Evolution in time	5
1.5	Illustration and analysis of the solution	5
2	A simple analytical solution	6

1 The problem (Reisenegger 2017)

1.1 PDF and initial conditions

In this section, the problem outlined in (reference to Reisenegger 2017) is being solved, namely, the growth of perturbation in the weak poloidal field \mathbf{B}_p in the presence of a strong background toroidal component \mathbf{B}_t . The approach of evolving \mathbf{B}_p boils down to numerically solving the following equation:

$$\frac{\partial \mathbf{B}_p}{\partial t} = -\nabla \times \left[\frac{1}{4\pi n} (\nabla \times \mathbf{B}_t) \times \mathbf{B}_p \right], \quad (1)$$

where the toroidal field \mathbf{B}_t can be decomposed using the basis vectors of the cylindrical coordinate system:

$$\mathbf{B}_t = 0 \cdot \mathbf{e}_R + B \cdot \mathbf{e}_\varphi + 0 \cdot \mathbf{e}_z. \quad (2)$$

The scalar function B in the expression above is defined as

$$B = (\chi_0/\chi)^2 = R^4 n^2, \quad (3)$$

$$n = 1 - r^2,$$

$$R = \sqrt{x^2 + y^2},$$

$$r = \sqrt{x^2 + y^2 + z^2}.$$

In the Cartesian coordinates' basis the toroidal field is presented in the form of

$$\mathbf{B}_t = -\sin \varphi B \cdot \mathbf{e}_x + \cos \varphi B \cdot \mathbf{e}_y + 0 \cdot \mathbf{e}_z$$

which is the same as

$$\mathbf{B}_t = -\frac{y}{R} B \cdot \mathbf{e}_x + \frac{x}{R} B \cdot \mathbf{e}_y + 0 \cdot \mathbf{e}_z.$$

It is assumed that the toroidal field does not evolve with time so that the curl of \mathbf{B}_t has to be computed just once, in the beginning of the simulation. Also, by the weakness of \mathbf{B}_p it is meant that $|\mathbf{B}_p| \ll |\mathbf{B}_t|$.

The initial configuration of the poloidal perturbation is the following:

$$\mathbf{B}_p|_{t=0} = 0 \cdot \mathbf{e}_R + 0 \cdot \mathbf{e}_\varphi + 10^{-7} \cdot \mathbf{e}_z. \quad (4)$$

The problem is solved on a 4π spherical shell-like manifold, where the radial variable r takes values from $r_{\min} = 0.5$ to $r_{\max} = 0.9$. As can be seen from the equations above, all relevant physical constants equal to 1 and the problem is treated in dimensionless variables.

1.2 First step. Solving for velocities

Firstly, the velocity field \mathbf{u} owing to the background toroidal magnetic field \mathbf{B}_t is calculated by merely taking curl of \mathbf{B}_t and then dividing the result by the scalar function $4\pi n$. It is done in a bit sophisticated manner though. Namely, in the first part, an auxiliary vector field $\mathbf{A} = 4\pi n \cdot \mathbf{u}$ is introduced, and the equation 5 below is solved:

$$4\pi n \cdot \mathbf{u} \equiv \mathbf{A} = -[\nabla \times \mathbf{B}_t]. \quad (5)$$

The calculations begins with use of a *trial function* \mathbf{w} , whereby the equation 5 is multiplied and then integrated over the whole domain. This is a classic procedure carried out in any numerical calculations that are somehow related to the finite element method. Henceforth we will omit writing the subscript t in the toroidal magnetic field \mathbf{B}_t in order to not confuse it with the vector components (i.e. B_k , where k are x , y and z). So, we rewrite the equation 5 in its integral form:

$$\int w_k A_k dV = - \int w_k e_{kij} \partial_i B_j dV, \quad (6)$$

where summation under the repeating indices is assumed and e_{kij} denotes the Levi-Civita tensor. After integrating by parts the right term we get

$$\int w_k A_k dV = - \int B_k e_{kij} \partial_i w_j dV + \int n_k e_{kij} w_i B_j dS. \quad (7)$$

The next step is to divide the manifold into cells and in each cell perform decomposition of \mathbf{w} and \mathbf{A} by means of *dealII* basic functions which are uniquely associated with nodes of the cells. These basis functions do not live on the real manifold of the problem, but lie on a so called reference manifold. In our numerical code when integrating something we use the Jacobian to go from one coordinate system, that charts the real manifold, to another coordinate system, that charts the reference manifold.

In the simplest and most convenient form, the decomposition would look like

$$w_k(\mathbf{x}) = \sum_l N_{kl}(\xi(\mathbf{x})) c_{kl}, \quad A_k(\mathbf{x}) = \sum_l N_{kl}(\xi(\mathbf{x})) d_{kl},$$

where $N_{kl}(\xi(\mathbf{x}))$ are the *dealII* basis functions, $c_{kl}(t)$ and $d_{kl}(t)$ are weights of the decomposition and ξ stands for coordinates in the reference manifold. In the sums l goes over all nodes of a cell within which the position vector \mathbf{x} is located. Note that there is no summation over k .

Actually, one can simplify this expression even further, if one recalls that each node has 3 degrees of freedom (because of three-dimensionality of the problem). Therefore, N_{kl} can be written as N_{3l+k} , where $3l+k$ is a unique number. For a cell, the maximum value of $3l+k$ represents the number of degrees of freedom in the cell, which is always three times larger than the number of nodes.

We can thus plug this decomposition expression into eq. 7, but now in the sum the index $a = 3l+k$ will cover not only degrees of freedom of a particular cell but that of the whole manifold (since the integration is performed over the entire manifold, not just one cell).

$$\sum_{l,m} \int N_{3l+k} N_{3m+k} c_{3l+k} d_{3m+k} dV = - \sum_l \int B_k e_{kij} N_{3l+j,i} c_{3l+j} dV + \sum_l \int n_k e_{kij} N_{3l+i} c_{3l+i} B_j dS, \quad (8)$$

Several things to note: [1] the sum over k in the first term on the left is also implied; [2] a comma in $N_{3l+j,i}$ represents a derivative of N_{3l+j} with respect to the i th spatial coordinate; [3] we can take the coefficients d and c out of the integrals.

The next step is to introduce a global matrix K_{ab} and a global vector F_a :

$$K_{ab} = \int N_a N_b dV, \quad F_a \equiv F_{3l+j} = - \int B_k e_{kij} N_{3l+j,i} dV + \int n_k e_{kji} N_{3l+j} B_i dS,$$

This step allows one to rewrite eq. 8 in the matrix-vector form:

$$c_a K_{ab} d_b = c_a F_a,$$

As the last equation has to hold true for any trial function \mathbf{w} (i.e. for any coefficients c_a), it immediately yields

$$\boxed{K_{ab} d_b = F_a} \quad (9)$$

The boxed equation is solved iteratively and the coefficients d_i are found. Following the calculation of the coefficients, the vector field \mathbf{A} is constructed and the velocity field $\mathbf{u} = \mathbf{A}/(4\pi n)$ is obtained. As calculated by our numerical code, the velocity field \mathbf{u} is depicted in figure 1.

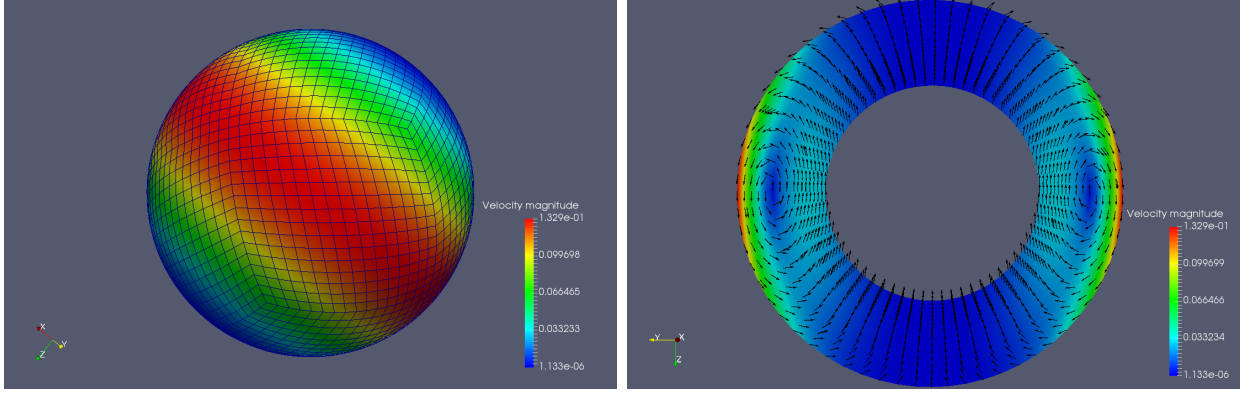


Figure 1: (left) Distribution of the velocity field \mathbf{u} on the outer surface of the spherical shell-like manifold. (right) A plane cut $x = 0$ of the same manifold, where the velocity field is shown. The arrows illustrate the tangent vectors to the field lines. The color describes the magnitude of the field (for both left and right panels).

1.3 Second step. Solving for poloidal perturbation

Now we seek for the solution of the partial differential equation

$$\frac{\partial \mathbf{B}}{\partial t} = \nabla \times [\mathbf{u} \times \mathbf{B}], \quad (10)$$

where from now on \mathbf{B} denotes the poloidal perturbation, not the toroidal magnetic field. Taking the same steps as in the subsection 1.2 we get

$$\int w_k \frac{\partial B_k}{\partial t} dV = \int w_i e_{ijk} \partial_j (e_{klm} u_l B_m) dV.$$

The term on the right hand side is integrated by parts

$$\int w_k \frac{\partial B_k}{\partial t} dV = \int (e_{ilm} u_l B_m) e_{ijk} \partial_j w_k dV - \int n_i e_{ijk} w_j (e_{klm} u_l B_m) dS, \quad (11)$$

and the deaIII basis function decomposition of \mathbf{B} and \mathbf{w} is fulfilled

$$w_k(\mathbf{x}, t) = \sum_l N_{kl}(\xi(\mathbf{x})) c_{kl}(t), \quad B_k(\mathbf{x}, t) = \sum_l N_{kl}(\xi(\mathbf{x})) d_{kl}(t).$$

Note, that here weights $c_{kl}(t)$ and $d_{kl}(t)$ are time-dependent.

The series representations of \mathbf{B} and \mathbf{w} are then plugged back into 11 and the equation is rewritten as

$$\begin{aligned} \sum_{p,s} \int N_{3p+k} N_{3s+k} c_{3p+k} \dot{d}_{3s+k} dV &= \sum_{p,s} \int (e_{ilm} u_l N_{3s+m} d_{3s+m}) e_{ijk} N_{3p+k,j} c_{3p+k} dV - \\ &- \sum_{p,s} \int n_i e_{ijk} N_{3p+j} c_{3p+j} (e_{klm} u_l N_{3s+m} d_{3s+m}) dS, \end{aligned} \quad (12)$$

where a dot over d denotes a time derivative. As the subsequent step, similarly to what has been done in the previous subsection, we write 12 in the matrix-vector notation

$$M_{ab} = \int N_a N_b dV, \quad K_{ab} \equiv K_{3s+m 3p+k} = \int e_{ilm} u_l N_{3s+m} e_{ijk} N_{3p+k,j} dV - \int n_i e_{ikj} N_{3p+k} e_{jlm} u_l N_{3s+m} dS.$$

The equation below has to hold true independently of the coefficients c_a

$$c_a M_{ab} \dot{d}_b = c_a K_{ab} d_b,$$

that leaves us with the following matrix-vector equation:

$$\boxed{M_{ab} \dot{d}_b = K_{ab} d_b.} \quad (13)$$

1.4 Third step. Evolution in time

Equation 13 now needs to be discretized in time. For this purpose the backward Euler is employed. The time then takes only discrete values:

$$d_b(t) \approx d_b(t_n) \equiv d_b^n,$$

where the upper index denotes a point along the time axis at which d_b is evaluated. Thus, at some point $t = t_n$ we have

$$M_{ab}^{n+1} \dot{d}_b^{n+1} = K_{ab}^{n+1} d_b^{n+1},$$

where it is assumed that both matrices can be time-dependent. The last steps are

$$\begin{aligned} \dot{d}_b^{n+1} &\approx \frac{d_b^{n+1} - d_b^n}{\Delta t} \\ M_{ab}^{n+1} \frac{d_b^{n+1} - d_b^n}{\Delta t} &= K_{ab}^{n+1} d_b^{n+1} \\ \boxed{(M_{ab}^{n+1} - \Delta t K_{ab}^{n+1}) d_b^{n+1} &= M_{ab}^{n+1} d_b^n} \end{aligned} \quad (14)$$

The equation 14 is solved iteratively in the code, the set of coefficients d_b is found and the poloidal perturbation is evolved in time by Δt . So, by numerically solving eq. 14 n times we obtain the solution at $t = t^{n+1}$ provided that the initial conditions are given.

1.5 Illustration and analysis of the solution

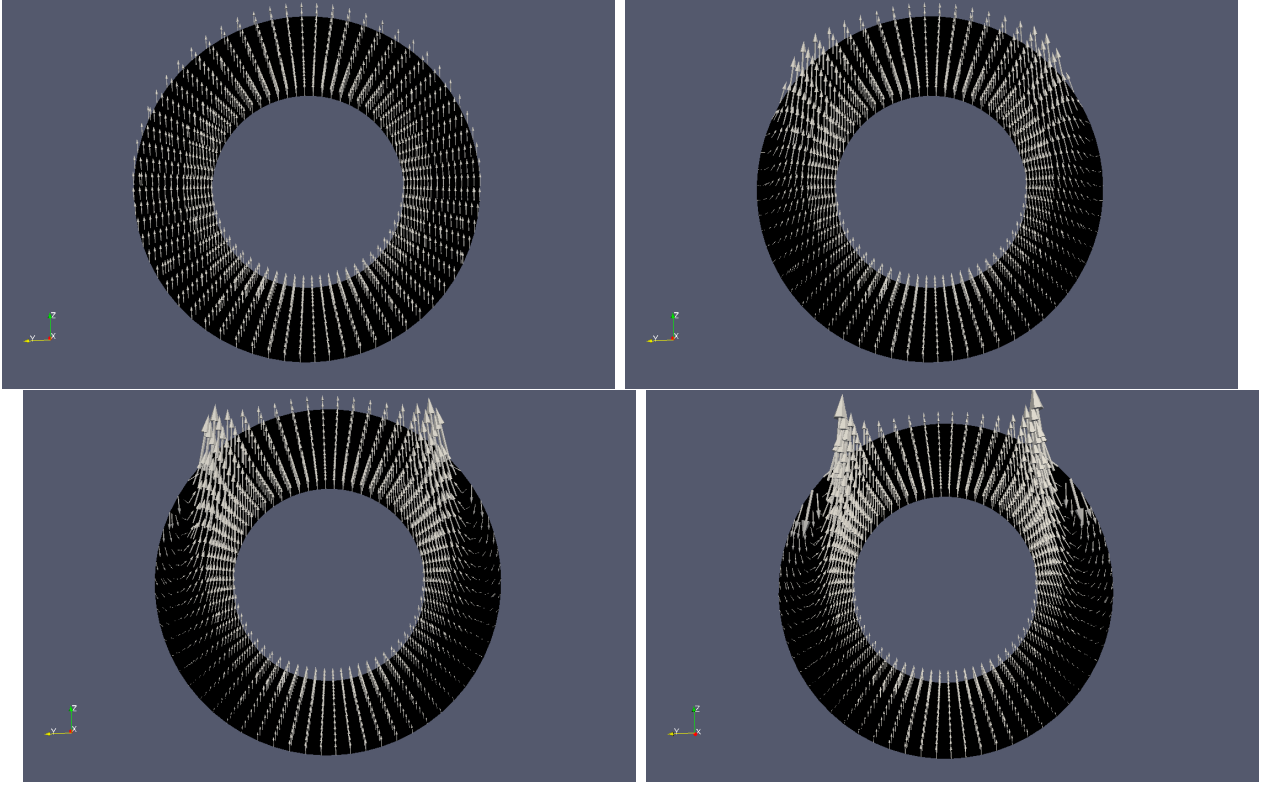


Figure 2: Four consecutive steps of evolution of the weak poloidal perturbation \mathbf{B}_p in the presence of the background toroidal component \mathbf{B}_t . The poloidal component \mathbf{B}_p on a plane cut $x = 0$ is shown. The arrows illustrate the vectors tangential to the field lines. Their size is linearly proportional to the magnitude of \mathbf{B}_p . The dimensionless time t has the following values: 0.0 (top left panel), 3.0 (top right panel), 5.0 (bottom left panel) and 6.5 (bottom right panel).

2 A simple analytical solution

If we now take

$$\mathbf{B}_t = -2y \cdot \mathbf{e}_x + 2x \cdot \mathbf{e}_y + 0 \cdot \mathbf{e}_z. \quad (15)$$

for the toroidal field and

$$\mathbf{B}_p|_{t=0} = e^z \cdot \mathbf{e}_x + 0 \cdot \mathbf{e}_y + 0 \cdot \mathbf{e}_z. \quad (16)$$

for the poloidal perturbation (which ironically does not look like poloidal anymore), equation 1 will have an analytical solution in the following form:

$$\mathbf{B}_p(t) = e^z e^{4t} \cdot \mathbf{e}_x + 0 \cdot \mathbf{e}_y + 0 \cdot \mathbf{e}_z. \quad (17)$$

In the left panel of figure 3 analytical and numerical solutions of equation 15 at different times t are shown. The number of degrees of freedom and DeaIII basis function order are varied. The right panel shows deviation of the numerical solution from the analytical solution as a function of the number of degrees of freedom at different times t . The deviation is defined as

$$\text{Deviation} = \max_{\text{nodes}} \left(\left| \frac{B_x^{\text{analytical}} - B_x^{\text{numerical}}}{B_x^{\text{analytical}}} \right| \right).$$

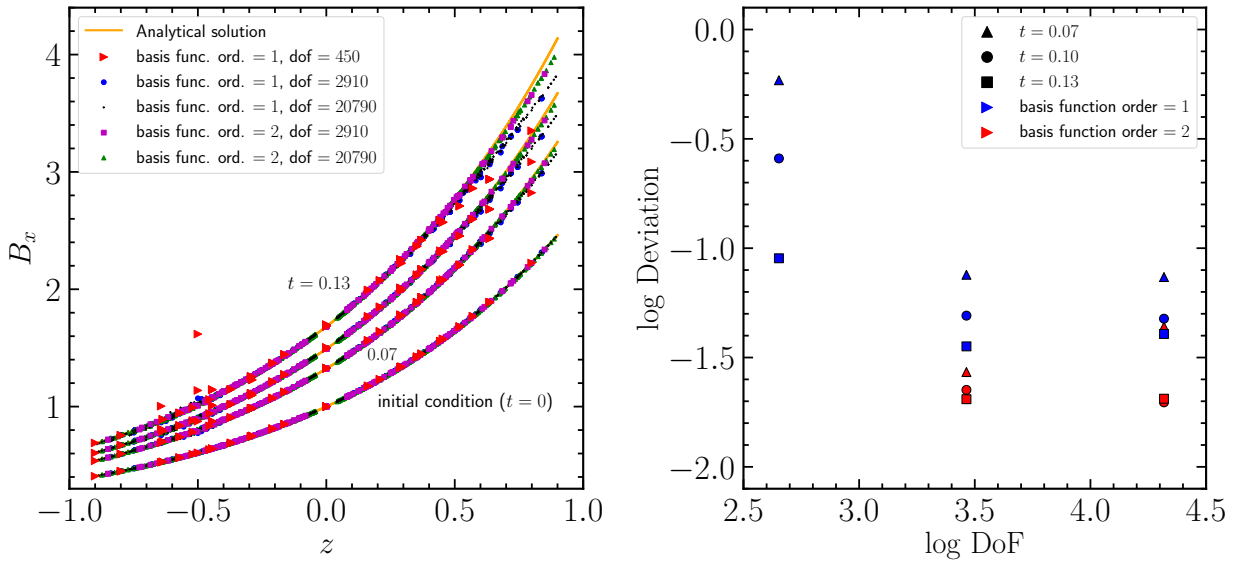


Figure 3: (*left*) Analytical and numerical solutions of equation 15 at different times t and for different number of degrees of freedom in the problem as well as DealII basis function order. (*right*) Deviation of the numerical solution from the analytical solution as a function of the number of degrees of freedom at different times t and for s DealII basis function order.